Freeform manufacturing of a microoptical lens array on a steep curved substrate by use of a voice coil fast tool servo

Sebastian Scheiding,[1,3,*] **Allen Y. Yi,**[2,4] **Andreas Gebhardt,**[1] **Lei Li,**[2] **Stefan Risse,**[1] **Ramona Eberhardt,**[1] **and Andreas Tünnermann**[1,3]

[1]*Fraunhofer Institute for Applied Optics and Precision Engineering Albert-Einstein-Str. 7, 07745 Jena, Germany*
[2]*Department of Integrated Systems Engineering, The Ohio State University 210 Baker Systems, 1971 Neil Ave, Columbus, Ohio 43210, USA*
[3]*Friedrich Schiller University Jena, Institute of Applied Physics, Jena, Germany*
[4]*yi.71@osu.edu*
**sebastian.scheiding@iof.fraunhofer.de*

Abstract: We report what is to our knowledge the first approach to diamond turn microoptical lens array on a steep curved substrate by use of a voice coil fast tool servo. In recent years ultraprecision machining has been employed to manufacture accurate optical components with 3D structure for beam shaping, imaging and nonimaging applications. As a result, geometries that are difficult or impossible to manufacture using lithographic techniques might be fabricated using small diamond tools with well defined cutting edges. These 3D structures show no rotational symmetry, but rather high frequency asymmetric features thus can be treated as freeform geometries. To transfer the 3D surface data with the high frequency freeform features into a numerical control code for machining, the commonly piecewise differentiable surfaces are represented as a cloud of individual points. Based on this numeric data, the tool radius correction is calculated to account for the cutting-edge geometry. Discontinuities of the cutting tool locations due to abrupt slope changes on the substrate surface are bridged using cubic spline interpolation.When superimposed with the trajectory of the rotationally symmetric substrate the complete microoptical geometry in 3D space is established. Details of the fabrication process and performance evaluation are described.

OCIS codes: (220.0220) Optical design and fabrication; (220.1920) Diamond machining; (220.4000) Microstructure fabrication; (240.3990) Micro-optical devices.

References and links

1. G. C Shin, I. W. Jung, V. Malyarchuk, J. Z. Song, S. D Wang, H. C. Ko, Y. G. Huang, J. S. Ha, and J. A. Rogers, "Micromechanics and advanced designs for curved photodetector arrays in hemispherical electronic-eye cameras," Small **7**, 851–856 (2010).
2. H. C. Ko, M. P. Stoykovich, J. Song, V. Malyarchuk, W. M. Choi, C.-J. Yu, J. B. Geddes, J. Xiao, S. Wang, Y. Huang and J. A. Rogers,"A hemispherical electronic eye camera based on compressible silicon optoelectronics," Nature **454**, 748–753 (2008).

#151593 - $15.00 USD Received 27 Jul 2011; revised 27 Aug 2011; accepted 27 Aug 2011; published 10 Nov 2011

3. D. F. Zhu, C. H. Li, X. F. Zeng, and H. G. Jiang, "Tunable-focused microlens arrays on curved surfaces," Appl. Phys. Lett. **16**, 081111 (2010).
4. K. H. Jeong, J. Y. Kim, and L. P. Lee, "Biologically inspired artificial compound eyes," Science **312**, 557–561 (2006).
5. J. G. Kim, N. Takama, B. J. Kim, and H. Fujita, "Optical-softlithographic technology for patterning on curved surfaces," J. Micromech. Microeng. **19**, 055017 (2009).
6. J. R. Nogues and R. L. Howell, "Fabrication of pure silica micro-optics by sol-gel process," Proc. SPIE **1751**, 214–24 (1993).
7. S. Scheiding, A. Y. Yi, A. Gebhardt, R. Loose, L. Li, S. Risse, R. Eberhardt and A. Tünnermann, "Diamond milling or turning for the fabrication of micro lens arrays: comparing different diamond machining technologies," Proc. SPIE **7927**, 79270N (2011), doi:10.1117/12.874751
8. T. A. Dow, M. H. Miller, and P. J. Falter,"Application of a fast tool servo for diamond turning of non-rotationally symmetric surfaces," Precis. Eng. **13**(4), 243–250 (1991).
9. C. F. Cheung, T. C. Kwok, S. To, W. B. Lee, X. Q. Jiang, and H. F. Li, "Measurement and characterization of surface quality in fast tool servo machining of optical microstructures," Key Eng. Mater. **381–382**, 517–520 (2008).
10. W. Gao, T. Araki, S. Kiyono, Y. Okazaki, and M. Yamanaka, "Precision nano-fabrication and evaluation of a large area sinusoidal grid surface for a surface encoder," Precis. Eng. **27**, 289–298 (2003).
11. A. Y. Yi, and L. Li, "Design and fabrication of a microlens array using slow tool servo," Opt. Lett. **30**(30), 1707–1709 (2005).
12. L. Li and A. Y. Yi, "Microfabrication on a curved surface using 3D microlens array projection," J. Micromech. Microeng. **19**, 105010 (8 pages), (2009).
13. F. Z. Fang, X. D. Zhang, and X. T. Hu, "Cylindrical coordinate machining of optical freeform surfaces," Opt. Express **16**(10), 7323–7329 (2008).
14. G. E. Davis, J. W. Roblee, and A. R. Hedges, "Comparison of freeform manufacturing techniques in the production of monolithic lens arrays," Proc. SPIE **7426**, 742605 (2009), doi:10.1117/12.824451
15. Factory accessory options, Nanotechnology Systems (2011), `http://www.nanotechsys.com/accessories/nanotech-450upl-factory-options`.
16. L. Li and A. Y. Yi, "Design and fabrication of a freeform prism array for 3D microscopy," J. Opt. Soc. Am. A **27**(12), 2613–2620 (2010).
17. R. Steinkopf, A. Gebhardt, S. Scheiding, M. Rohde, O. Stenzel, S. Gliech, V. Giggel, H. Löscher, G. Ullrich, P. Rucks, A. Duparre, S. Risse, R. Eberhardt, and A. Tünnermann, "Metal mirrors with excellent figure and roughness," Proc. SPIE **7102**, 71020C (2008), doi:10.1117/12.797702

1. Introduction

Accurate optical components for beam shaping, imaging and diffraction of light can now be manufactured by established processes such as ultraprecision machining. In addition to fabrication of metal mirrors, lenses or two-dimensional (2D) - gratings, diamond tools can also be utilized to create three-dimensional (3D) microoptical structures. As a result, geometries that are difficult or impossible to readily manufacture using $2\frac{1}{2}$-D lithographic techniques such as photo-, gray tone or laser lithography may now be fabricated by use of ultraprecision machining using relatively small diamond tools of a few to few hundreds μm with well defined cutting edges. 3D microlens arrays have potential applications in compact compound eye imaging devices, machine vision, and robotic motion control systems. Compared to its larger size counterpart such as a wide angle optical lens, a 3D microlens array divides the signal spatially without delays thus providing visual information immediately to either an observer or a machine controller.

Microstructures on 3D substrates have unique applications in opto-electronic devices. However processes to create these features have been limited. In some recent publications, Rogers et al. developed a 3D process aimed at creating flexible electronics. In their approach, photosensing units were first created on a stretched substrate made of PDMS using conventional 2D lithographic process. After the devices were fabricated on the stretched planar surface, the substrate is then allowed to relax back to its original shape, which was a hemisphere [1, 2].

Zhu [3] and Lee [4], using different but in principle largely similar processes, i.e., first built the flat devices then attached the flexible substrates on a curved substrate to create microlens

#151593 - $15.00 USD Received 27 Jul 2011; revised 27 Aug 2011; accepted 27 Aug 2011; published 10 Nov 2011

arrays or an artificial compound eye model. Kim et al. recently also demonstrated a process involves in complex steps of thin film coating, patterning and replicating of micropatterns on cylindrical surface [5]. Much earlier, Howell described a sol-gel process of replicating silica microoptics that can be made to match the mold surface [6] which could be applied to 3D microfabricaiton. These efforts although innovative but have limitations either in production rate, substrate geometry, pattern feature selection or the combination of these problems. The studies involving 3D microfabrication demonstrated an urgent need for a more robust, flexible and also cost effective and production ready process.

Partially as a complimentary approach to lithographic processes used for 3D microfabrication, ultraprecision diamond machining using well defined micro cutting edges were popular in creating microstructure on flat substrates [7–10]. More recently efforts to apply slow tool servo ultraprecision diamond machining technique to creating 3D microstructures have also been reported [11–13]. Using slow tool servo technique, complex optical geometries over a large surface area can be created with surface finish adequate for some optical applications. However tool marks due to large step size and relatively low production rate because of limitations on slide speed are yet to be resolved. While slow tool servo has been the primary choice for manufacturing freeform optical surfaces with large deviations, fast tool servo was mainly utilized for small peak-to-valley microfeature fabrication due to limit in travel on most fast tool servo designs [14].

Although the techniques aforementioned are unique and creative, still a robust, multi-scale, low cost but readily available production method has not been identified. This study is an attempt to provide an answer to these needs. In addition, the proposed process can be applied to many common engineering materials thereby providing the community with a much needed tool for complex 3D geometry on arbitrary substrate fabrication. The newly available high frequency, high dynamic range voice coil fast tool servo development ensures that this process can be easily adjusted for rapid prototyping optical devices that were not available before. The creative interpolation using spline reported in this publication is a critical step that allows precise 3D microstructures of optical quality to be created.

2. Freeform machining technology

Ultraprecision diamond turning machines are routinely used to fabricate optics with a center of symmetry. However recent developments in optical design require 3D structures with no rotational symmetry, but rather high frequency asymmetric features. These optics are treated as freeform geometries because the machining process applied is similar to that of an arbitrary surface. Typical deviations from the rotationally symmetric reference features such as a sphere range from a few μm to mm or higher are manufactured on an ultraprecision lathe with additional strokes of the machining tool. The stroke of the diamond tool is synchronized to the angular and radial position of the freeform surface on the machine's workpiece spindle. The forward and reverse motion is achieved either by the mechanical axes (i.e., Slow Tool Servo - STS), or an additional kinematic tool holder of a low inertia device (Fast Tool Servo - FTS) [14].

For high frequency freeform geometries the FTS technology is generally preferred. An FTS system can be powered by either a piezo or a voice coil actuator. Piezo driven systems offer the advantage of higher peak acceleration and bandwidth compared to voice coil systems but are limited in travel to several to several hundred μm. For microoptics fabrication a piezo actuated FTS-system was generally considered a better approach compared to a voice coil system. In this research the intent was to show that a properly designed, commercially available FTS-system of voice coil design is equally capable of achieving robust performance for fabrication of micro optics with a high precision true shape and low micro roughness. To our best knowledge, this has not been verified at the scale reported in this research. In addition, one of the goals is to

#151593 - $15.00 USD Received 27 Jul 2011; revised 27 Aug 2011; accepted 27 Aug 2011; published 10 Nov 2011

demonstrate that production ready manufacturing process can be derived from this research without major modifications to the equipment used.

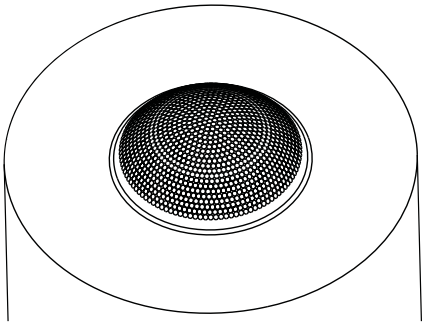

Fig. 1. Geometry of the 3D microlens array containing 1,219 spherical lenslets. The clear aperture of the lens area is 19 mm and the outside diameter of the substrate is 40 mm.

For the microlens array investigated in this study, a Nanotech 450 UPL machine with an additional NFTS-6000, from Moore Nanotechnology Systems, LLC was used. The maximum stroke of the FTS is ± 3 mm. The integrated linear scale encoder with sub- nm resolution is in a closed control loop with a voice coil actuator to position the air bearing slide in real time. The NFTS-6000 is able to precisely follow an amplitude of 100 μm at 160 Hz with maximum acceleration of 49.1 $\mathrm{m/s^2}$ [15].

To demonstrate the full potential of microoptics fabrication using freeform manufacturing technique, a microlens array design with a high frequency asymmetric portion was selected. The overall microlens array design shown in Fig. 1 is an optical mold insert for an injection molding tool. The molded plastic lens array can be used as a 3D microoptical imaging element to transfer features from a 3D mask onto a curved substrate using lithographic process [12] or as part of a microoptical device [16]. The mold insert contains 1,219 single spherical lenslets whose vertices are arranged on a spherical surface. The design data of the microlens array are summarized in table 1.

Table 1. Geometry of the Microlens Array on a Steep Curved Substrate

Total number of lenslets	1,219
Radius of curvature of the lenslets	-3.808 mm (concave)
Vertex pitch circle radius	11 mm (convex)
Span angle α	2.6026°
Maximum slope angle	60°
Outer diameter	9.5 mm

#151593 - $15.00 USD Received 27 Jul 2011; revised 27 Aug 2011; accepted 27 Aug 2011; published 10 Nov 2011

3. Programming the freeform tool path

The programming of the FTS can either be accomplished using commercial CAM-Tools such as NanoCAM 3D or proprietary software solutions. Although commercial software solutions are well developed for a wide variety of standard freeform machining applications, major drawbacks are the limited number of data points and possible approximation errors coming from numerical interpolation of high frequency freeform surfaces. The limitation of the number of data points leads to an increased distance between the control nodes, which subsequently results in higher shape deviation and surface roughness for high frequency freeform surfaces. Typical spline interpolation errors are transitions between piecewise differentiable surfaces where spline-ringing may occur. Due to the above mentioned limitations of the commercial software, a proprietary software solution using MATLAB programming was developed to process the data into an appropriate format for machining. The freeform data to control the FTS-System is stored in a look up table in the form of the center points of the diamond tool in polar coordinates. The streaming of data into this look up table allows the computing of large point cloud data files containing millions of center nodes of the tool.

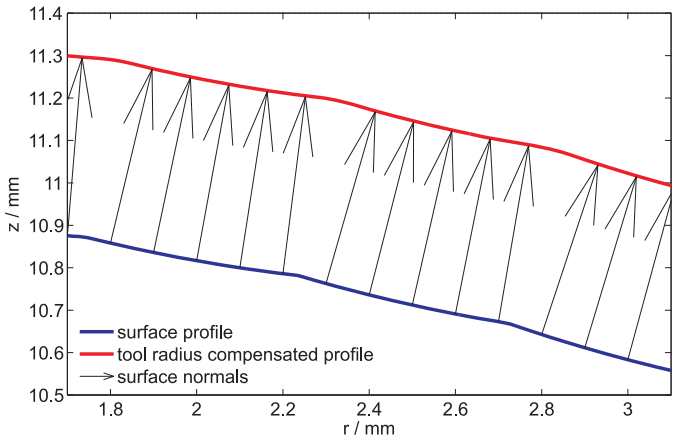

Fig. 2. Tool radius compensation of the diamond tool tip in the radial direction. The number of surface normals is reduced for clarity.

To transfer the 3D surface data with the high frequency freeform features into a numerical code for machining, the piecewise differentiable surface is calculated in 25.2×10^6 supporting points in a polar mesh. The maximum supporting point distance was chosen not to exceed 5 μm in any direction of the array to assure a precise representation of the shape. Therefore the elements are equally spaced with an incremental size of 4.75 μm along the radial direction and with an angular incremental of $360^\circ/12,600$. The point spacing in the angular direction depends on the fixed angular increment and the radial position of the node. Hence the supporting point density of the lenslets decreases with increasing substrate radius.

While a lenslet on the outer diameter is well described with 5,575 supporting points, the central microlens is over-determined with 63,000 surface nodes. This high number is not necessarily needed for the processing of the central lenslet, but needed to describe the entire array in one common uniform polar mesh. Based on these point cloud data, the tool radius corrections are made to account for the cutting-edge geometry. Typically in diamond turning applications tool radius corrections are only done in the radial direction. The cutting edge radius of the diamond tool tip in the angular direction is in the range of 10 Å – 20 Å therefore can be neglected. Figure 2 shows the tool radius correction for one of the 12,600 lines. Due to the discontinuities

#151593 - $15.00 USD Received 27 Jul 2011; revised 27 Aug 2011; accepted 27 Aug 2011; published 10 Nov 2011

in the slope of the profile, radius compensation is not defined in the transition area between the spheres. The missing points have to be calculated using an interpolation scheme. Either a linear or a spline based interpolation can be applied to fill in the missing data.

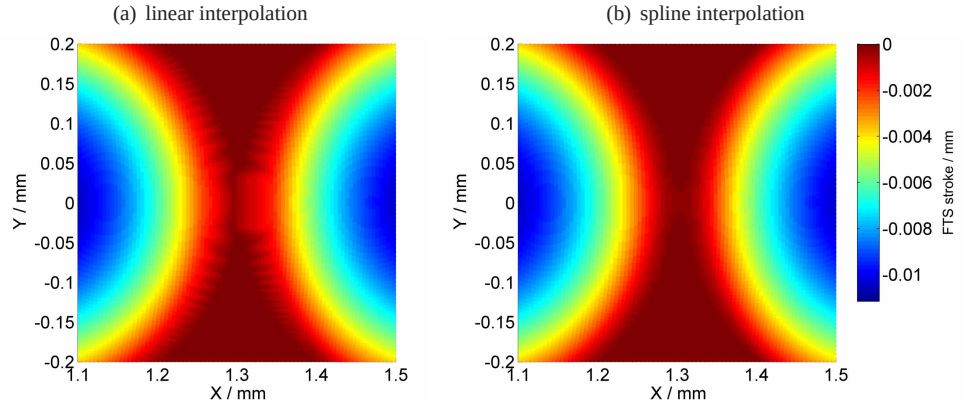

Fig. 3. Different interpolation methods to calculate the tool center points from the surface nodes.

The difference between a spline based approach and a linear interpolation is illustrated in Fig. 3. The linear interpolation leads to sharp discontinuities in the radius corrected surface as a result of the discontinuous slope of the design surface. The spline based interpolation bridges these gaps based on the surface slopes of the neighboring nodes. Hence a continuous and smooth edge of the lenslets is expected.

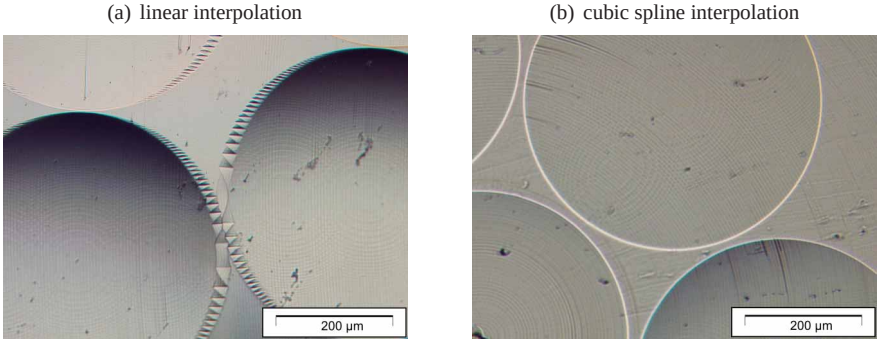

Fig. 4. microscopic image of the surface texture as the results of two different interpolation methods.

Figure 4 shows microscopic images of the diamond turned surface using the aforementioned interpolation methods. The linear interpolation leads to serrated edges of the lenslets as displayed in Fig. 3(a) and subsequently was verified in experiment as shown in Fig. 4(a). The step height of the microstructure ranges around 200 nm. A smooth boundary of the lenslets is shown in Fig. 4(b). Here the cubic spline interpolation method is used to smooth the boundaries of the piecewise differentiable surfaces. This interpolation method increases the computational load by a factor of 9 compared to the linear interpolation. The average calculation time for one of the 12,600 radial lines of the polar mesh is 2.18 µs.

The difference between the spline interpolated tool path used for the fabrication of the microlens array and a much denser description of the same surface is shown in Fig. 5. This error

#151593 - $15.00 USD Received 27 Jul 2011; revised 27 Aug 2011; accepted 27 Aug 2011; published 10 Nov 2011

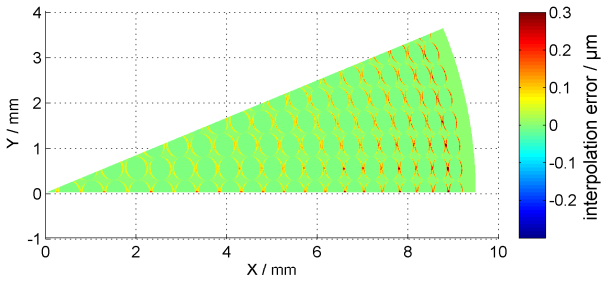

Fig. 5. calculated error map of 1/8 of the entire array for spline based interpolation of the tool path.

map, which represents 45° of the array, approximates the deviations caused by the spline interpolation. The figure shows that both the microlens surfaces and the overall sphere are precisely defined by the cutting location data. Errors occur in the regions close to the edges of the lenslets. The tool path overshoots due to the discontinuous slope that is bridged with the cubic spline interpolation in the radial direction. Depending on the supporting point density this effect becomes larger with an increasing substrate radius to a maximum value of 510 nm (p-v). The contribution to the overall shape error is 33 nm (rms). The interpolation accuracy could be improved by a finer mesh of the tool path at the cost of longer computational time and machining time due to the limited data transfer rate.

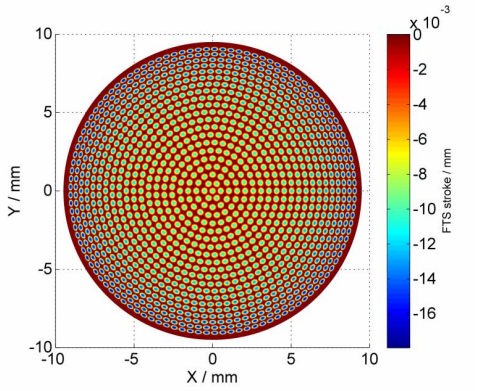

Fig. 6. FTS tool path generation for fabrication of the microlens array on a curved surface.

The surface compensated for tool radius of the curved array is subsequently split into a rotationally symmetric- and a freeform part. The linear slides of the ultraprecision machine are employed to machine the rotationally symmetric share, while the FTS system, which is a redundant kinematic is used to structure the high-frequency freeform surface. The separation is typically based on subtracting the identified best fit rotationally symmetric surface from the point cloud data. In the presented work, the overall substrate radius and the tool radius were subtracted from the point cloud data. The complete freeform portion of the tool center points is shown in Fig. 6. Superimposed with the curved trajectory of the rotationally symmetric portion the geometric information for this microoptical component is established.

#151593 - $15.00 USD Received 27 Jul 2011; revised 27 Aug 2011; accepted 27 Aug 2011; published 10 Nov 2011

4. Cutting parameters for freeform machining

The total FTS-stroke needed to fabricate the lens array is 18 μm. According to the frequency response specification of the manufacturer, the FTS can be operated at more than 200 Hz at this amplitude. Assuming a constant spindle speed, the highest necessary frequency of the FTS is expected on the outer diameter. Here 109 lenslets are machined on a common reference circle. The possible speed of 110 rpm is reduced to 25 rpm, because the excitation of 18 μm does not follow a sinusoidal motion. Moreover constraints to the cutting parameter are given by the limited data transfer rate of the FTS-control, which is used in a streaming mode. $7,500$ lines$/$s can be processed by the FTS-system. Because the angular increment is $360^\circ/12,600$ the maximum spindle speed for the calculated polar mesh is 35.7 rpm. To achieve a reasonable smooth surface, the feed per revolution is adjusted to 5 μm. The cutting data are summarized in Table 2.

Table 2. Cutting Parameter for the Freeform Machining of the Microlens Array

Cutting Data	
Diamond tool radius	0.470 mm
Clearance angle	12°
Include angle	60°
Depth of cut	< 18 μm
Spindle speed	25 rpm
Feed rate	0.125 mm$/$min
Feed per rev.	5 μm

The freeform microlens array is machined using a two-tool configuration. The first diamond tool was used for rough cutting of the sphere and the reference surfaces, the second tool was mounted on the FTS unit and was used to cut the hemisphere with the spherical microlenses. The machining time for the finish cut using the FTS is 80 min. The material used is a high strength aluminum alloy as mold inserts for injection molding.

Fig. 7. A finished freeform microlens array mold insert containing 1,219 single spherical lenslets.

#151593 - $15.00 USD Received 27 Jul 2011; revised 27 Aug 2011; accepted 27 Aug 2011; published 10 Nov 2011

5. Results of the freeform machining

Upon completion of the freeform machining using the fast tool servo process, the microlens array was cleaned and inspected. The finished 3D microlens array is shown in Fig. 7. The microlens array was first measured for surface roughness using a white light interferometer and then for geometry using the Panasonic Ultra Accuracy 3D-Profilometer (UA3P). Finally, the microlenses were also evaluated using a Twyman-Green interferometer for optical performance due to form deviation and micro surface roughness from machining.

5.1. Micro surface roughness

For characterizing the micro roughness, a Zygo white light interferometer NewView 600 with a $\times 50$ objective lens and a numerical aperture of 0.55 was used. To distinguish between form error and roughness profile a spherical surface with a radius of 3.8082 mm was subtracted from the measured data. The surface texture is shown in Fig. 8. The finish of less than 4 nm (rms) is similar to conventional ultraprecision diamond turning of aluminum alloys [17]. The influence of the FTS system's dynamics is visible in the high frequency residues in both directions.

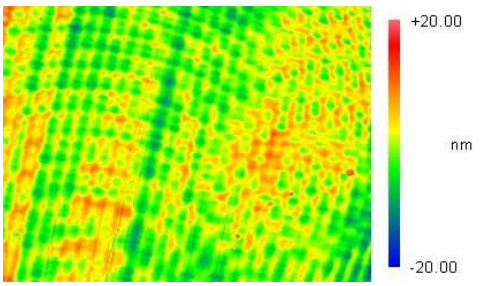

Fig. 8. Micro roughness of the aluminum surface inside a lenslet in a field of 140 μm x 110 μm measured with Zygo NewView 600 white light interferometer after subtraction of a best fit sphere is 3.9 nm (rms), 44 nm (p-v).

5.2. Form error

The shape deviation of the complete freeform surface is measured with the tactile 3D-profilometer UA3P-5 from Panasonic. This measurement device, with a measurement range of 200 mm $\times$ 200 mm $\times$ 45 mm, uses a diamond stylus tool with a tip radius size of 2 μm to scan the surface. The accuracy over the measurement range is 100 nm in X,Y directions, with a repeatability of 50 nm. The probe measurement accuracy depends on the slope of the object. For slopes up to 30° the accuracy of the installed UA3P is below 50 nm. Since the piecewise differentiable surface topology is not programmable in the UA3P proprietary software, the profilometer is used to scan the surface only. The 3D profile is acquired by scanning concentric circles from the middle of lens at the vertex to the reference flat outside of the clear aperture of the entire array. The radius feed of the concentric circles is 50 μm. Every 30 μm along the profile, a measurement point is recorded. The dense measurement path assures a proper shape description of the high frequency freeform surface. The exported point cloud, representing the center points of the contact probe with a radius of 2.02 μm on the surface, is fitted and recalculated to obtain the shape error image as shown in Fig. 9. The surface slopes for the radius correction of the diamond stylus are calculated using the design data of the freeform lens array.

The shape of this high frequency freeform surface of 3D microlens array deviates well below ± 3 μm (p-v) from the design surface. The measured shape error is 1.37 μm (rms). The overall

#151593 - $15.00 USD Received 27 Jul 2011; revised 27 Aug 2011; accepted 27 Aug 2011; published 10 Nov 2011

(a) overall shape deviation

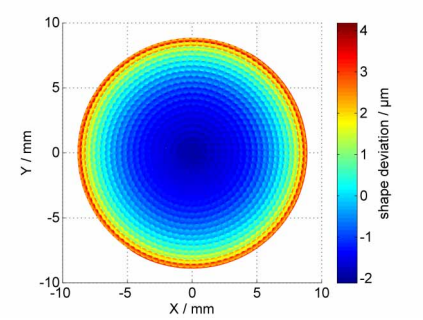

(b) shape deviation (rotationally symmetric portion)

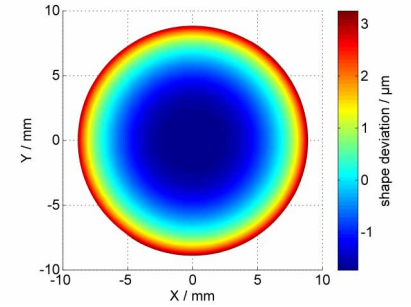

(c) shape deviation (non rotationally symmetric portion)

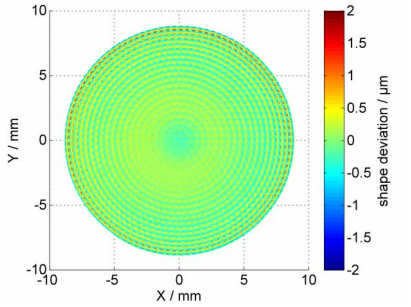

Fig. 9. Shape Deviation from the design freeform surface measured with the 3D profilometer UA3P (Panasonic). The overall shape error is the sum of a rotationally symmetric error (4.5 µm p-v) and a non rotationally symmetric error (2 µm p-v, 237 nm rms).

shape error as shown in Fig. 9(a) can be separated into a rotationally symmetric part and a freeform error portion as shown in the Figs. 9(b) and 9(c). Geometry errors result in focal point shift and non-rotationally symmetric errors result in high order aberrations. The reason for the rotationally symmetric error share is a slight radius error of the overall sphere, whose origin is the inaccurate radius value during the tool setting. Majority of these errors can be minimized by adjusting tool setting during machining. In addition, error compensation can also be implemented in cutting tool path for further improvements. The freeform error image shown in Fig. 9(c) is a sum of different error sources such as the dynamic behavior of the fast tool servo, thermal influences during the cutting process, the waviness of the tool cutting edge and also an inaccurate radius value. The form error on the peripheral lenses is slightly higher than other lenses mainly due to the inaccurate tool radius value, which causes a position error of these microlenses. Further contributions are caused by the overshooting of the FTS, less point spacing density of the tool path and increased interpolation errors. For most applications where microlens arrays are used, the errors in these microlenses can be safely ignored. Nonetheless, continuing investigation of the nature of this error and the remedies is being performed and relevant results will be included in the future publications.

The surface deviation, measured with the Zygo white light interferometer is shown in Fig. 10. The deviation of the measured surface from a best fit sphere is shown. The image is a section of a lenslet on the outer diameter of the array. It shows the boundary of that particular lenslet. The profile in Fig. 10(b) shows the cross section of that microlens. The influence of the inertia

#151593 - $15.00 USD Received 27 Jul 2011; revised 27 Aug 2011; accepted 27 Aug 2011; published 10 Nov 2011

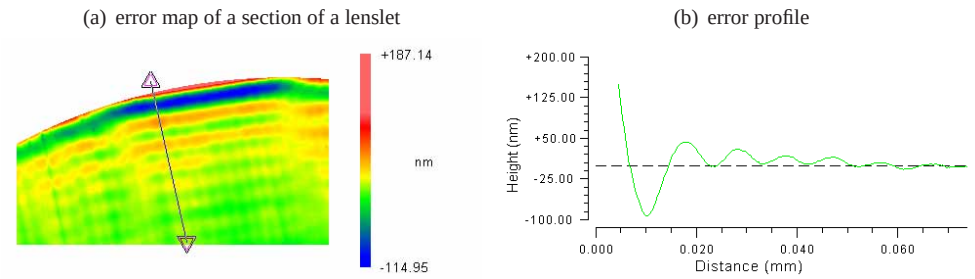

Fig. 10. Surface deviation from the spherical surface inside a lenslet on the outer diameter of the array shows the dynamic behavior of the FTS system. The surface was measured with a white light interferometry.

of the FTS system can be observed in the high frequency deviations in the lenslets, where the displacement of the FTS changes at the highest frequency. Here the FTS system overshot up to 150 nm at a spatial frequency of 100 mm^{-1} in the areas near the lenslet on the edge of the microlens array. The frequency and the magnitude of the deviations increased versus the paraxial area of the lens array.

5.3. Optical characterization

The individual microoptics were evaluated using a self-built Twyman-Green interferometer with a He-Ne laser (633 nm). Figure 11 shows the optical path difference (OPD) map of three of the microlenses on the machined mold insert. Figure 11(a) shows the OPD map of the microlens at the center of the microlens array and Fig. 11(b) the OPD map of the microlens in the middle of the array the Fig. 11(c) the OPD map of a microlens on the edge of the microlens array. Due to the radial position difference, which results in different tool path codes, the OPD maps also showed different patterns. Figure 11(a) has a symmetric pattern because the tool path for the microlens at the center is also symmetric. Figure 11(b) shows an asymmetric pattern and the aberration along the X direction (or the radial direction) is higher because the tool path for this microlens is a series of curves along the Y direction (angular direction). Figure 11(c) shows even higher asymmetricity and the aberration along the X direction. Table 3 lists the aberration of these three microlenses measured using the Twyman-Green interferometer. The RMS value for the microlens at the center is less than 1/20 λ and the RMS value for the microlens at the edge is about 1/16 λ, indicating high quality microlenses. The values in Table 3 were calculated based on the measured optical path difference (OPD) maps. The OPD map reflects the difference of the microlens surface with a perfect spherical surface. Theoretically, the shape accuracy can be derived by combining the OPD data with a precision translation stage to measure the radius of that perfect sphere.

#151593 - $15.00 USD Received 27 Jul 2011; revised 27 Aug 2011; accepted 27 Aug 2011; published 10 Nov 2011

(a) microlens at the center of the array

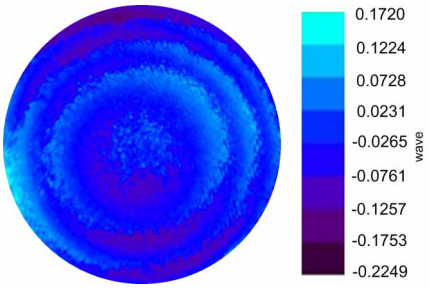

(b) microlens in the middle of the array

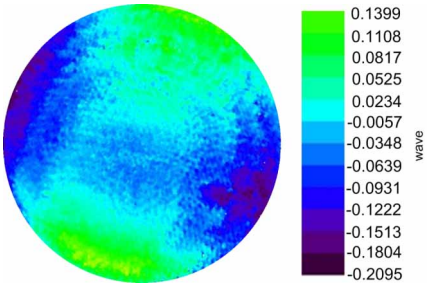

(c) microlens on the edge of the array

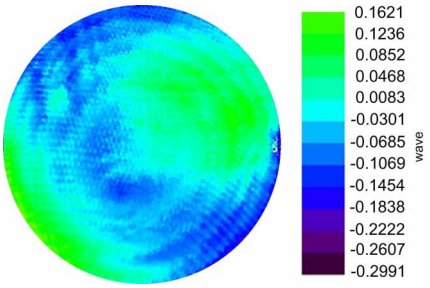

Fig. 11. Optical path difference map of the microlenses measured by using Twyman-Green interferometer.

6. Conclusion

For 3D freeform geometries that are difficult or impossible to manufacture using other technologies, FTS can be an excellent alternative. However, freeform machining using FTS can be challenging in terms of tool path programming. The FTS used in this research has a wide enough dynamic range for machining high frequency freeform surfaces. The design selected in this study is an excellent representation for a wide variety of freeform microoptics. Consequently the challenges in manufacturing included the mathematical description of the entire surface as a point cloud in a polar mesh as well as the tool radius compensation of the piecewise differentiable surfaces. A cubic spline based approach to bridge the neighboring microlenslets was thoroughly investigated and proven to be very effective.

The overall cycle time of 80 minutes for finishing machining the described high strength aluminum alloy injection mold insert and the surface quality of < 4 nm (rms) demonstrate an excellent suitability of the freeform machining process based on the voice coil driven FTS for structuring of these small optics. The shape deviations in the μm-range are adequate for some

#151593 - $15.00 USD Received 27 Jul 2011; revised 27 Aug 2011; accepted 27 Aug 2011; published 10 Nov 2011

Table 3. Summary of Aberration Measurements using a Twyman-Green Interferometer

Parameter (wave)	microlens @ center	microlens @ middle	microlens @ edge
PV 98 %	0.2236	0.3082	0.3013
RMS	0.0452	0.0660	0.0633
X Astigmatism	0.0648	-0.1106	0.0458
Y Astigmatism	-0.0340	-0.1023	-0.1082
X Coma	-0.0288	0.0122	-0.0813
Y Coma	0.0491	0.0178	0.0577
Spherical	-0.0070	-0.0096	-0.0156

imaging optics and for a broad spectrum of illumination optics. Correction cycles to improve the shape of the optical element after a metrology step were not included in this study for high frequency freeform surfaces, because the major contributions to the shape irregularities are caused by the inertia of the FTS system and inconsistent cutting conditions over the diameter of the workpiece. The minimum radius of curvature will be determined by the size of the diamond tool. A practical limit is about 2 μm cutting radius therefore curvature less than this value cannot be fabriccated. Another issue is when the overall part size or the deviation increases, accuracy of the tool paths will decrease due to dynamic behavior of the cutting tool. Last but not the least, interpolation scheme is always a critical issue in securing the final contour accuracy.

Geometries can be machined by this process are mainly limited by the diamond cutting tool design. By increasing the clearance angle up to 40°, the practical limit of a precision diamond tool, and reducing the radius of the diamond tool used, geometries with finer features across large deviations can be fabricated. The limitation on maximum deviation of this approach is determined by the magnitude of the nonsymmetrical deviation of the substrate surface due to maximum voice coil travel (± 3 mm in this report), another limitation is due to the fact that the substrate materials need to be diamond turnable for this process to work. For applications, devices utilizing 3D microlens arrays suffer reduced lateral resolution, i.e., the acuity of the 3D microdevices will be severely diffraction limited if the size of the microlenses is small. In addition, crosstalk among the neighboring lenslets is also an issue that requires delicate solutions.

This study nonetheless clearly demonstrated that freeform machining can realize its great potential as a complementary approach to lithography for structuring three-dimensional optics at the micro and meso scale. In addition, the process studied in this research seamlessly combines the conventional diamond machining for overall geometry and high speed machining of micro features in an uninterrupted operation thereby providing a systems solution to a variety of industrial problems.

As part of future investigation, replication by injection molding or other mass production methods can efficiently and economically reproducing these geometries. For injection molding of polymer microlens arrays, there will be issues related to the replicated plastic components such as form deviation due to packing and cooling and stress birefringence in the molded parts.

#151593 - $15.00 USD Received 27 Jul 2011; revised 27 Aug 2011; accepted 27 Aug 2011; published 10 Nov 2011

Acknowledgments

The authors acknowledge the financial support by the Fraunhofer Society that enabled the collaboration between the Fraunhofer Institute for Applied Optics and Precision Engineering (IOF) and the Ohio State University by the Fraunhofer program Prof X^2.

This research is also partially based on work supported by National Science Foundation under Grant No. CMMI-0928521 and EEC-0914790. Any opinions, findings, and conclusions or recommendations expressed in this material are those of the authors and do not necessarily reflect the views of the National Science Foundation.

#151593 - $15.00 USD Received 27 Jul 2011; revised 27 Aug 2011; accepted 27 Aug 2011; published 10 Nov 2011